ELSEVIER

Microporous and Mesoporous Materials 53 (2002) 97–108

MICROPOROUS AND MESOPOROUS MATERIALS

www.elsevier.com/locate/micromeso

Crystallization and Si incorporation mechanisms of SAPO-34

Juan Tan *, Zhongmin Liu *, Xinhe Bao, Xianchun Liu, Xiuwen Han, Changqing He, Runsheng Zhai

State Key Laboratory of Catalysis, Dalian Institute of Chemical Physics, Chinese Academy of Science, Dalian 116023, China

Received 23 November 1999; accepted 12 February 2002

Abstract

In this study of the synthesis of SAPO-34 molecular sieves, XRD, SEM, XRF, IR and NMR techniques were applied to monitor the crystalloid, structure and composition changes of the samples in the whole crystallization process in order to get evidence for the crystallization as well as Si incorporation mechanism of SAPO-34. XRD results revealed that the crystallization contained two stages. In the first 2.5 h (the earlier stage), high up to ~80% of relative crystallinity could be achieved and the crystal size of SAPO-34 was almost the same as that of any longer time, indicating a fast crystallization feature of the synthesis. In this stage, IR revealed that the formation of SAPO-34 framework structure was accompanied by the diminution of hydroxyls, suggesting that crystal nuclei of SAPO-34 may arise from the structure rearrangement of the initial gel and the condensation of the hydroxyls. NMR results reveal that the template and the ageing period are crucial for the later crystallization of SAPO-34. Preliminary structure units similar to the framework of SAPO-34 have already formed before the crystallization began (0 h and low temperature). Evidence from IR, NMR, and XRF shows that the formation of the SAPO-34 may be a type of gel conversion mechanism, the solution support and the appropriate solution circumstance are two important parameters of the crystallization of SAPO-34. Meanwhile, NMR measurements demonstrated that about 80% of total Si atoms directly take part in the formation of the crystal nuclei as well as in the growth of the crystal grains in the earlier stage (<2.5 h). Evidence tends to support that Si incorporation is by direct participation mechanism rather than by the Si substitution mechanism for P in this stage (<2.5 h). In the later stage (>2.5 h), the relative content of Si increased slightly with a little decrease of Al and P. The increase of Si(4Al) and the appearance of the Si(3Al), Si(2Al), Si(1Al) and Si(0Al) in this stage suggest that substitution of the Si atoms for the phosphorus and for the phosphorus and aluminum pair takes place in the crystallization. The relationship among structure, acidity and crystallization process is established, which suggests a possibility to improve the acidity and catalytic properties by choosing a optimum crystallization time, thus controlling the number and distribution of Si in the framework of SAPO-34.

Keywords: Mechanism; Molecular sieves; SAPO-34; Synthesis; Characterization

1. Introduction

SAPO-34, a novel molecular sieve in the SAPO family, has been attracting much attention in catalytic applications due to its small pore character and medium acidic strength property [1–3]. One of

* Corresponding authors. Tel.: +86-411-4685510; fax: +86-411-4691570.

E-mail addresses: tanjuan@dicp.ac.cn (J. Tan), zml@dicp.ac.cn (Z. Liu).

1387-1811/02/$ - see front matter
PII: S1387-1811(02)00329-3

the most remarkable prospects of SAPO-34 is its excellent performance in catalytic conversion of methanol and/or dimethylether to light olefins (MTO/DTO) [4–6]. Thus, it provides a potential for developing a commercial MTO/DTO process to produce light olefins from coal or natural gas, other than by the conventional oil routes [7–9]. Many works [10,11] were reported on the acid properties of SAPO-34 and its application as catalyst, however, the relations between acid properties and catalytic performances are still not clear enough for most reaction systems. The Brønsted acid sites of SAPO-34 are attributed to the introduction of Si atoms into the neutral $AlPO_4$-34 framework. From the viewpoints of the references [12–16], it is proposed that Si atoms incorporate into the $AlPO_4$-34 structure by two different substitution mechanisms: the first, denoted as SM1, is that the Si substitution for phosphorus form Si(4Al) entities, which gives rise to negative charges for forming Brønsted acid sites; the second mechanism (SM2) is the double substitution of neighboring aluminum and phosphorus by two silicon atoms to form Si(nAl) ($n = 3$–0) structures, which leads to the formation of stronger Brønsted acid sites. The structure, acidity and catalytic property of SAPO-34 depend on the number and distribution of Si in the framework [16–18], which is closely related to the synthesis process, i.e., to the crystallization and Si incorporation mechanisms. However, the synthesis mechanism and the relations among mechanism, structure and acidity of SAPO-34 have not been established.

In the present work, crystallization as well as silicon incorporation mechanism of SAPO-34 has been studied by monitoring the whole synthesis process with various techniques such as XRD, SEM, XRF, IR, and NMR. The results of synthesis and characterization were correlated to investigate the diversification of the structure and the composition with the crystallization time. This study was expected to provide evidence to understand the crystallization and Si incorporation mechanisms of SAPO-34 and the theoretical basis for the improvement of the catalyst. Moreover, it will also be beneficial for the understanding of the synthesis and property of other SAPO molecular sieves.

2. Experimental

SAPO-34 was prepared based on a hydrothermal method described in the patent [19] from a gel composition of $3R{:}0.6SiO_2{:}Al_2O_3{:}1.6H_3PO_4{:}50H_2O$, where R is the template. The sources of the framework elements were pseudoboehmite, 85% phosphoric acid, silica sol (25%), water and triethylamine (TEA). The mixing of the starting materials to form a gel was in an order of, H_3PO_4, silica sol, distilled water and template, during which half amount of distilled water was added to pseudoboehmite in the first mixing step. The gel mixture was removed to a 2 l stainless-steel autoclave. After ageing for 24 h, the initial gel was heated and crystallized at 200 °C under autogenic pressure with stirring. Samples at different crystallization time were withdrawn periodically from the autoclave during the synthesis process by a home-made apparatus. Some gel samples were filtered and retained for studies. The solid "as-synthesized" samples were then obtained after filtration, washing by water for at least four times and dried at 110 °C for 12 h. These samples, unless stated otherwise, were used for various characterizations by many techniques. Some of the as-synthesized samples were calcined in air at 550 °C for 3 h to remove the template and water.

X-ray power diffraction patterns were recorded on a RIGAKU D/max-rb instrument using Cu Kα radiation with a nickel filter. SEM photographs were obtained on a HITACHI S-3200N scanning electron microscope. X-ray fluorescence analysis (XRF) was performed on a Bruker SRS 3400 X-Ray Spectrometer using AG Rh 66-G0.75 μm radiation operating at 30 kV. Lines were Kα1, Kα1, and Kα1 for Al, P and Si, respectively. IR spectra of the samples in the region of the framework stretching vibrations (300–4000 cm^{-1}) were measured using KBr containing pellets on a Perkin–Elmer 983G IR spectrophotometer. ^{13}C, ^{29}Si, ^{31}P, ^{27}Al CP/MAS and MAS NMR spectra were carried out on a Bruker DRX-400 spectrometer. Spinning speeds were 4, 4, 4, and 8 kHz for ^{13}C, ^{29}Si, ^{31}P, and ^{27}Al, respectively, and chemical shifts are quoted respectively from DDS (3-trimethylsiyl propanesulfonic acid sodium salt), DDS, 85% phosphoric acid, and $Al(H_2O)_6^{3+}$. Short radio-fre-

quency pulses 1/20 was used for the ^{27}Al spectra to ensure that the measurements were quantitatively reliable.

3. Results and discussion

3.1. Crystalline analysis

The X-ray diffraction patterns are presented in Fig. 1, the crystallization curve according to the relative crystallinity in Fig. 2, and the SEM photographs in Fig. 3. First of all, it should be pointed out that for all as-synthesized samples with evident relative crystallinity, their XRD patterns were confirmed in agreement with that of SAPO-34 reported in the literature [1]. This proved that the synthesis was reliable.

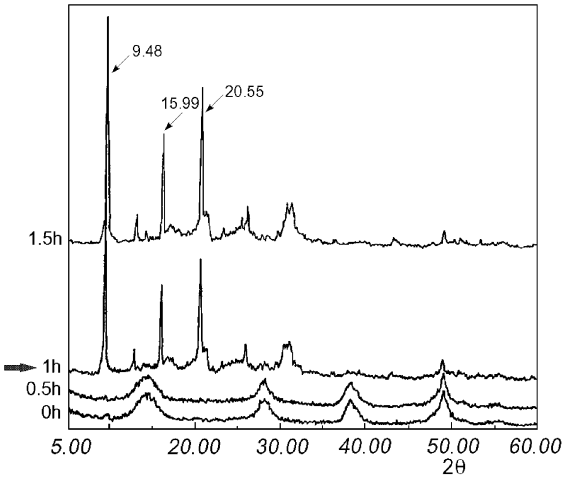

Fig. 1. XRD spectra of as-synthesized samples.

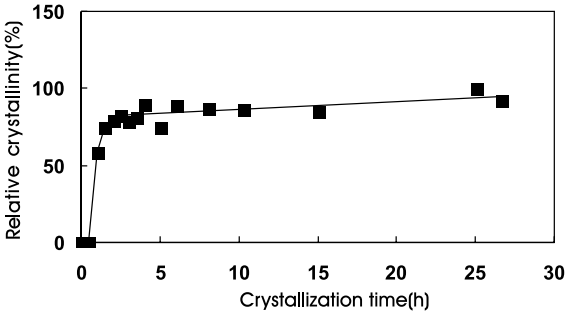

Fig. 2. Crystallization curve of SAPO-34.

XRD results showed that the whole crystallization process contained two stages, the earlier stage (<2.5 h) and the later stage (>2.5 h). In the initial period of the earlier stage, i.e., before first 0.5 h, no characteristic peaks of SAPO-34 could be observed, indicating that there was only an amorphous phase in the synthesis system. After 1 h, the crystallization became evident and the relative crystallinity increased rapidly with time. High up to ~80% relative crystallinity could be achieved at 2.5 h, confirming fast crystallization character of the synthesis. In the later stage (>2.5 h), although the crystallization time was longer than the earlier stage, the increase of relative crystallinity was smaller.

SEM results (Fig. 3) were in agreement with XRD data. In the initial period of crystallization (<0.5 h), only amorphous phase was observed. This period can be ascribed to the induction period of the crystal nuclei. With the increase of the crystallization time, cubic SAPO-34 crystals appeared and the crystals became larger. After 1 h, the SEM photograph showed that cubic SAPO-34 crystals appeared, which coexisted with amorphous phase, while the crystals was distributed in a range, with an average size of about 1.6 μm. At the end of the earlier stage (2.5 h), the amorphous phase disappeared and the SAPO-34 crystals were well distributed with a size of 3 μm. In the later stage (>2.5 h), similar to the change of relative crystallinity, the size of the crystals changed only a little even after a 26 h crystallization. However, the cubic SAPO-34 crystals became more regular than in the earlier stage.

3.2. Infrared spectral analysis

Infrared spectra of the as-synthesized samples in the framework vibration frequency region are shown in Fig. 4. The various vibration frequencies (Table 1) have been assigned, based on relevant reports [14,15].

Though there are no obvious change in the first 0.5 h in the XRD spectra, IR spectra clearly showed that structure changes have taken place in the solid part of the gel in the nucleation process.

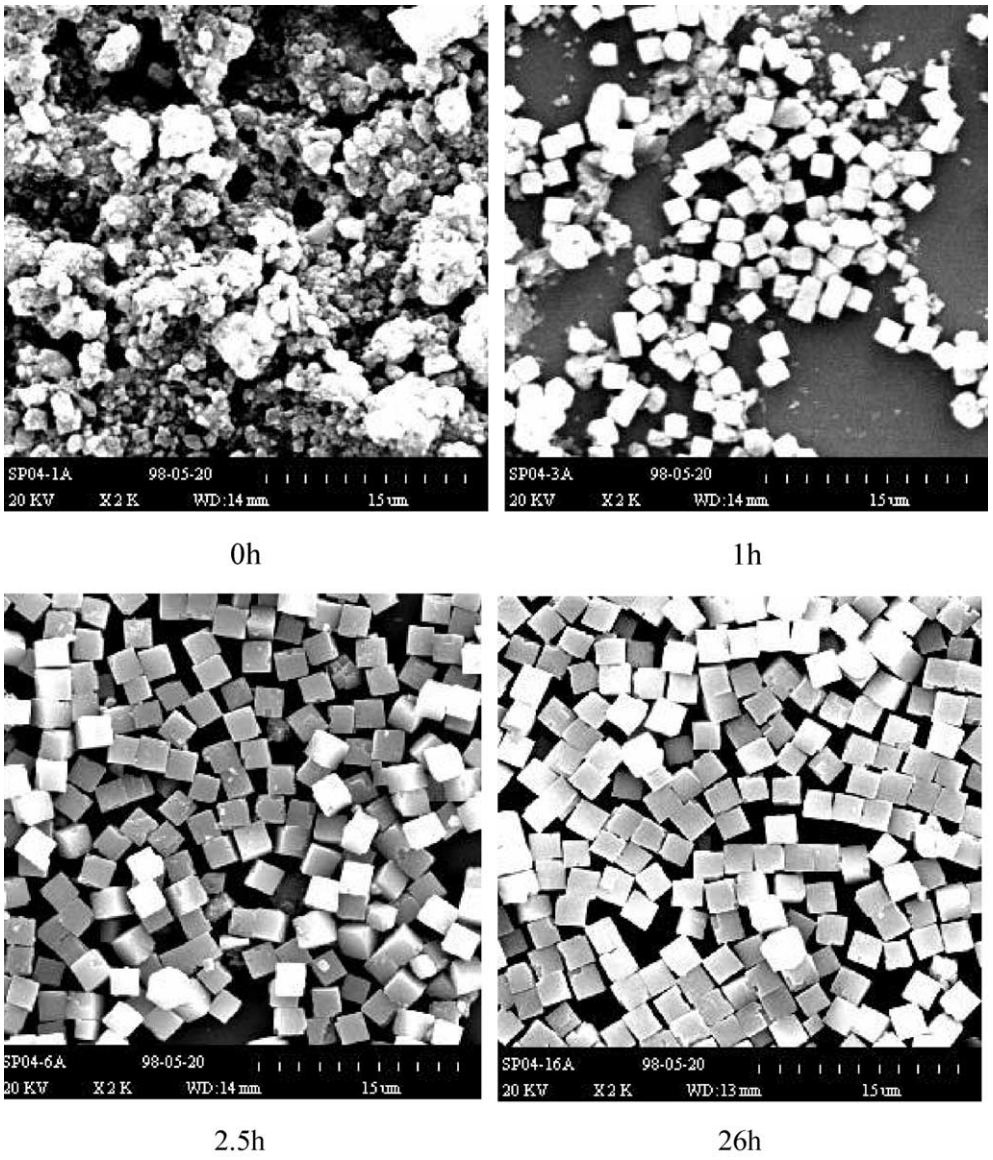

Fig. 3. SEM images of as-synthesized samples.

According to the spectra and the assignments, it can be seen clearly that the characteristic peaks of the amorpha (785, 618, 520, 365 cm^{-1}) transferred to broad peaks in 0.5 h. After 1 h, the characteristic peaks of the SAPO-34 (635, 530, 480, 380 cm^{-1}) appeared and increased, which match very well with those of the XRD and the SEM. These suggest a change of composition and a structure rearrangement in the nucleation process. It indicates that the crystal nuclei of SAPO-34 arise from the structure rearrangement of the initial gel to the crystal lattice. Moreover, it was observed obviously that the disappear of the stretch band of Si–O (785 cm^{-1}) and transfer of the bending band of SiO_4 (470 cm^{-1}) in the solid phase of the initial gel, which indicates evidently that the silicones directly

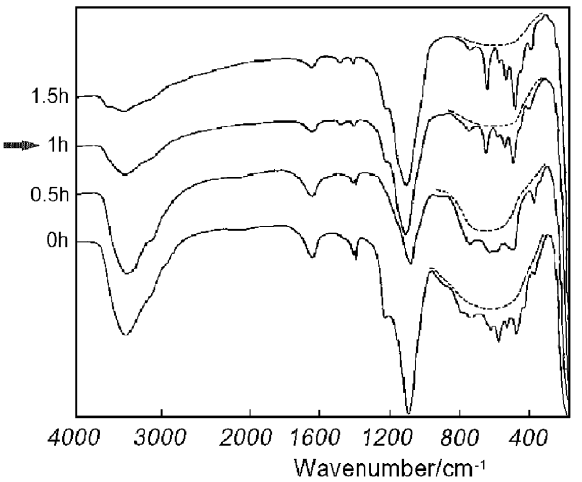

Fig. 4. IR spectra of the as-synthesized samples in the earlier stage of crystallization.

take part in the SAPO-34 nucleation. In addition, an alternate interpretation is that the Si species exist as silica colloid at $t = 0$ h which is more ordered in the gel phase and is broken up into several SiO_x species at $t = 0.5$ h giving rise to the observed broad peaks which sharpen in the crystalline material at $t > 1.0$ h.

In the initial gel, the Si, P, and Al species are in hydration states, which caused hydroxyl vibrations that could be observed on the IR spectra. The stretch bands (3000–3650 cm^{-1}), the bending bands (1550–1650 cm^{-1}) and the vibration bands (400–800 cm^{-1}) of the hydroxyls decreased in time indicating the nucleation process is a structure rearrangement, accompanied by the condensation of the hydroxyls.

3.3. NMR analysis

Fig. 5 shows the ^{27}Al, ^{31}P and ^{29}Si NMR spectra of the as-synthesized samples in the earlier stage of crystallization (<2.5 h). It illustrated clearly that the ^{27}Al, ^{31}P and ^{29}Si NMR spectra changed very little in the first 0.5 h. As there were only amorphous Al, P and Si in the initial gel, the ^{27}Al NMR showed a single resonance at 8 ppm that could be assigned to hydrated aluminum oxide. Meanwhile, ^{31}P and ^{29}Si NMR spectra presented broadened resonance region indicating varied and disordered states of P and Si in the gel phase. After 1 h, the characteristic resonance peaks of SAPO-34 appeared. ^{27}Al NMR showed a typical NMR peak at 38 ppm due to aluminum in tetrahedral environment of the SAPO-34 framework. ^{31}P and ^{29}Si NMR each showed a single resonance at −27.4 and −90.5 ppm, respectively, typical of P(Al) and Si(4Al) environments in the SAPOs [14,15,20–23]. With the consumption of the amorphous materials with time, the resonance peaks of tetrahedral aluminum, P(Al) and Si(Al) in the SAPO-34 lattice increased rapidly with the decrease of the resonance peaks of the amorphous materials, indicating higher crystallinity of the samples. At 2.5 h, the resonance at 8 ppm in the ^{27}Al NMR shifted to 12 ppm that can be assigned to six-coordinated Al due to extra linkages of tetrahedral Al to –OH groups, deriving from either the template or the hydrolysis of water, which indicated the finish of the crystallization.

In addition, ^{31}P and ^{29}Si NMR clearly showed that there were weak resonance peaks at the same chemical shift of P(4Al) and Si(4Al) of SAPO-34 in

Table 1
Assignment of the IR bands in framework vibration region of the as-synthesized samples

Crystallization time (h)	Structure type	Asymmetric stretch		Symmetric stretch		T–O bend					
		P–O–Al (P–O–P)	O–P–O	Si–O	P–O (Al–O)	D-6 rings	PO_4	$(Si,Al)O_4$	SiO_4	Rings	Channel
0	Amorpha	1225	1090	785	730	–	618 570	520	470	365	–
0.5	Amorpha	–	1070	–	730	–	618 570	–	475	365	–
1	Crystal	1215	1100	–	730	635	570	530	480	–	380
1.5	Crystal	1215	1100	–	730	635	570	530	480	–	380

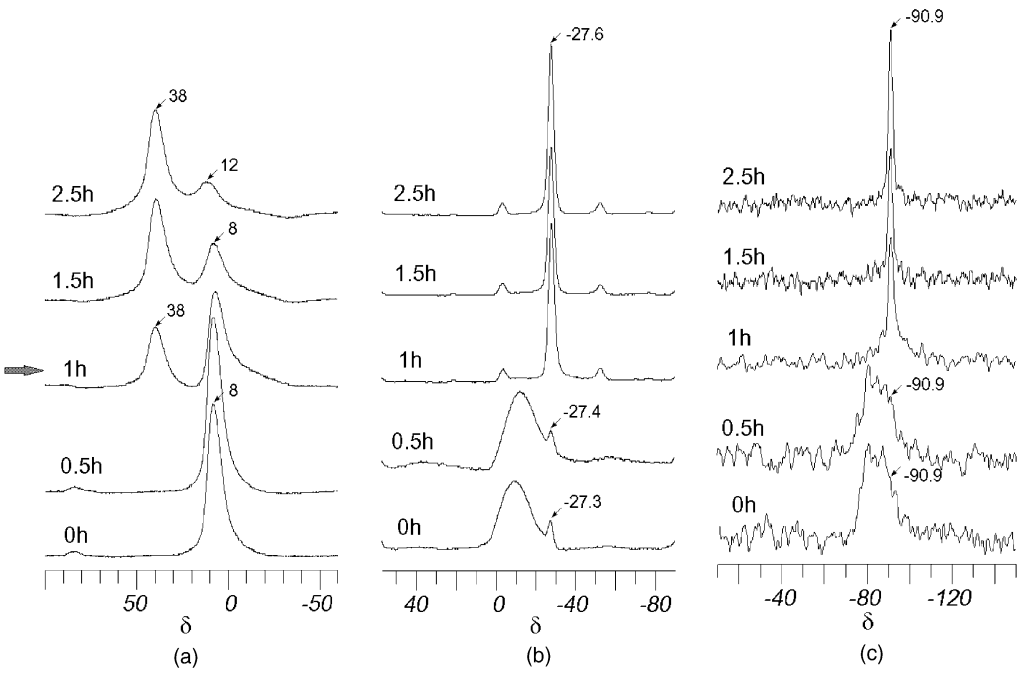

Fig. 5. ^{27}Al MAS (a), ^{31}P MAS (b) and ^{29}Si CP/MAS (c) NMR spectra of as-synthesized samples in the earlier stage of crystallization.

the first 0.5 h. As the template and water influenced greatly the coordination manner of Al, the samples in the earlier stage of crystallization were calcined and dehydrated at 550 °C for distinguishing clearly the difference between the sample of 0 h and the alumina source. The result in Fig. 6 matched well with those of the ^{31}P and ^{29}Si NMR in Fig. 5. There is a weak resonance at 38 ppm with the same shift of tetrahedral Al in the SAPO-34 framework for the first 0.5 h.

^{27}Al, ^{31}P and ^{29}Si NMR results reveal that the template and the ageing period are crucial for the later crystallization of SAPO-34. Structure changes take place in the starting gel during the ageing period after the addition of the template [24]. It clearly shows that "preliminary structure units" similar to the framework of SAPO-34 have already formed before the crystallization began (0 h and low temperature). These structure units are likely the precursor of the crystal nuclei of SAPO-34.

So, it can be inferred that one of the important steps occurring during the ageing period, that is the partial dissolution or depolymerization of the silica colloid, which is promoted by the alkaline conditions come from the template [24]. In the alkaline gel, the dissolved silica is reactive which react with $Al(OH)_4^-$ and PO_4^{3-} species to produce "preliminary structure units". When the crystallization temperature was raised, the crystallization began, the preliminary structure units condensed to "secondary building units", then the crystal nuclei of SAPO-34 formed. The evidences of NMR spectra directly show that a small quantity of silica colloid have been broken down to smaller more reactive species in the ageing period. When the crystallization began, the condensation of the structure units made the equilibrium moving which lead to more silica colloid broke down and the reactive Si species directly take part in the crystal nucleation and crystal growth.

The ^{27}Al and ^{31}P NMR spectra changed very little in the later stage of crystallization (>2.5 h), while the ^{29}Si NMR changed greatly (Fig. 7). At 10 h, four weak resonance signals appeared at −94.4, −99.6, −104.3 and 109.8 ppm, which can be assigned to Si(3Al), Si(2Al), Si(1Al) and Si(0Al), respectively, [13–15] suggesting that small amount of Si atoms are incorporated into the SAPO-34

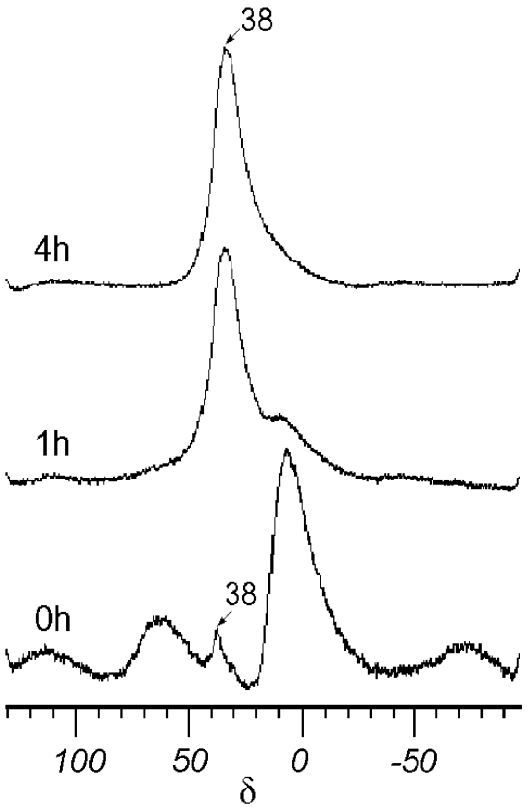

Fig. 6. ^{27}Al MAS NMR spectra of calcined and dehydrated samples in the earlier stage of crystallization.

framework by the substitution mechanism in this stage.

3.4. Crystallization mechanism

The spectroscopic evidences of the solid samples showed that the preliminary structure units of SAPO-34 firstly formed in the gel, which inferred that the crystal nuclei might arise from the gel phase. More evidence were taken from the XRF and ^{13}C MAS NMR results.

The XRF results (Fig. 8) showed that there was a great change of the chemical composition of the solid samples in the period of 0.5–1.5 h. After 1.5 h, the change of chemical composition of the as-synthesized samples became much slow. Comparison of XRD results (Fig. 2) and Fig. 8 showed that the relative composition of the sample at 1 h approached closely to the crystal composition, but the relative crystallinity of the sample was not very high (about 58.3%). It revealed that the composition changes of the reaction mixture took place faster than the crystallization process in this stage, implying a mass transition between the solution phase and the gel phase had already occurred in preparation for the growth of the crystals. This phenomenon also suggests that the initial crystals

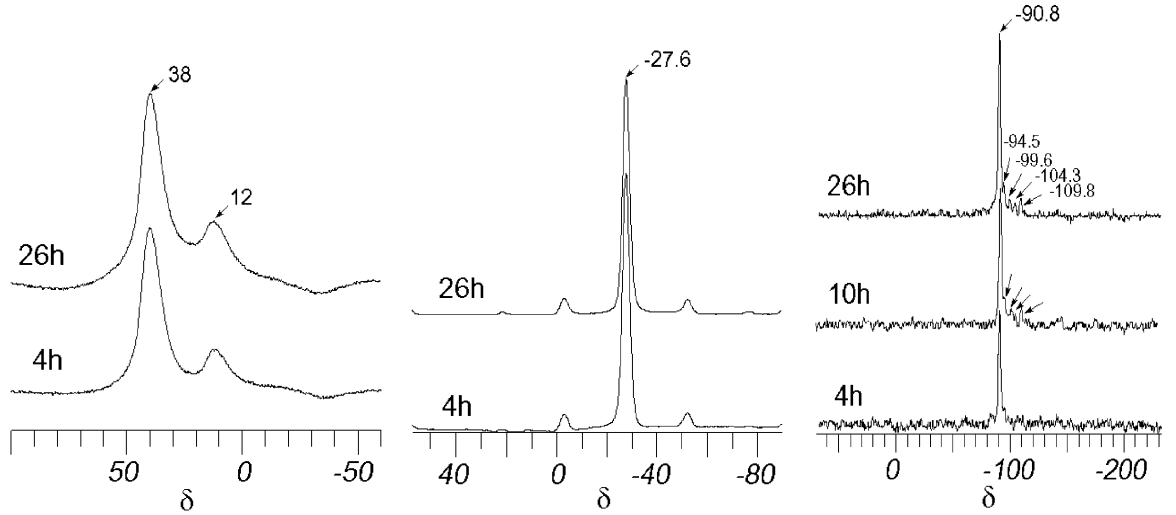

Fig. 7. ^{27}Al MAS (a), ^{31}P MAS (b) and ^{29}Si CP/MAS (c) NMR spectra of as-synthesized samples in the later stage of crystallization.

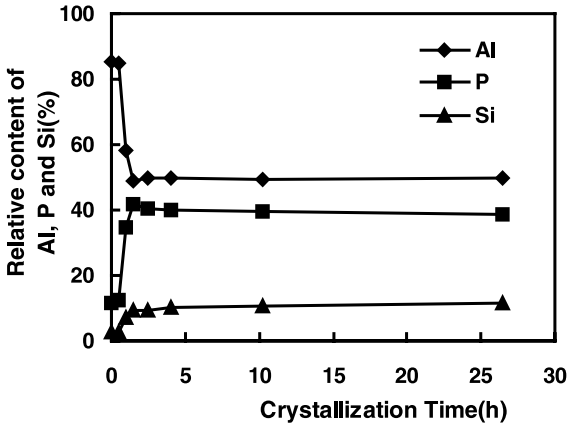

Fig. 8. Influence of crystallization on the composition of solid samples.

(crystal nuclei) may arise from the gel phase, and the solution phase with mass transferring to the gel phase may provide the source for the growth of crystal grains.

Calculation from the ^{13}C MAS NMR results of the solid samples (Fig. 9) showed that the relative content of template (TEA) in the solid samples increased gradually with time, which was similar to the change of relative crystallinity. The relative slow change of the template content with time (comparison with the composition change) gives another evidence of mass transfer between the gel and the solution phase. Meanwhile, little template was found in the first two samples (0–0.5 h). A reasonable explanation is that the template is captured in the crystals of SAPO-34, before the formation of the crystals, the interaction between the template and the gel phase is very weak. In fact, it was observed that in the preparation of final mixture, the addition of the template caused a great change of the solution composition (Fig. 10). This phenomenon demonstrates a strong action of the template in the solution phase. This action

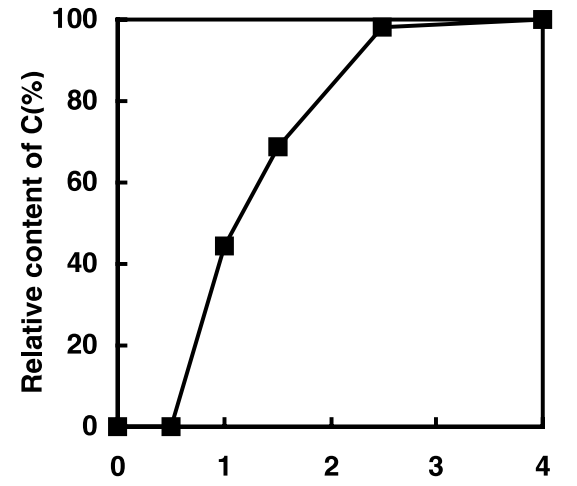

Fig. 9. Relative content curve of template in the as-synthesized samples.

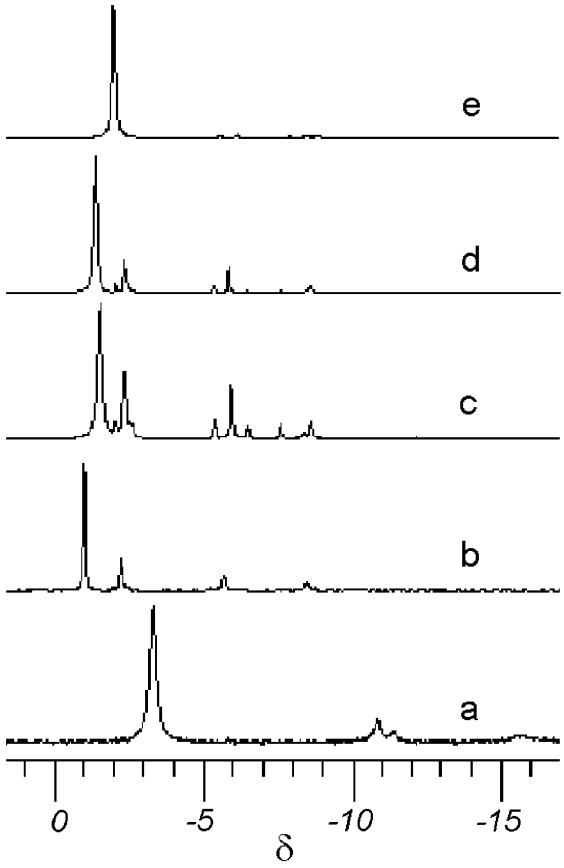

Fig. 10. Liquid ^{31}P NMR of the liquid samples in the first steps of the crystallization process. (a) Liquid sample of the stirred mixture of the raw sources (silica sol, pseudoboehmite, orthophosphoric acid and water). (b) Liquid sample of the reaction mixture of the raw sources and template (TEA). (c) Liquid sample of the reaction mixture after ageing (the initial state of the crystallization, 0 h). (d) Liquid sample of the reaction mixture crystallized for 2.5 h. (e) Liquid sample of the reaction mixture crystallized for 26 h.

became stronger obviously after ageing while weakening in the crystallization process, suggesting the influence of the template and ageing for the solution circumstance which is another important factor for the synthesis of SAPO-34.

These results from IR, NMR, and XRF give evidence that the formation of the SAPO-34 may be a type of gel conversion mechanism, the solution support and the appropriate solution circumstance are two important parameters of the crystallization of SAPO-34.

3.5. Mechanism of Si incorporation into SAPO-34 framework

During the whole crystallization process, the ^{27}Al, ^{31}P and ^{29}Si MAS NMR spectra of as-synthesized samples were splinted and integrated to calculate the relative content of Al(IV), P(IV) and Si(IV) incorporation into the framework of SAPO-34. Changes of the relative contents of Al, P and Si in the whole crystallization were shown in Fig. 11a. In the earlier stage (<2.5 h) of the crystallization, only Si(4Al) was found in the structure, and the increase of the relative contents of Si, P and Al in the framework of the as-synthesized samples showed a similar trend as that of the crystallinity, which was different from those in the later crystallization stage (>2.5 h). The relative content of Si increased slightly with slight decrease of Al and P in the later stage (>2.5 h). Results of IR and NMR reveal that Si atoms directly take part in the crystal nucleation in the induction period of crystallization (<0.5 h). After 1 h, Si atoms directly incorporated into the framework of SAPO-34 by the participation of crystallization to form the Si(4Al) structure, of which the relative content was about 40%, contrast to that of the highest sample. Then the relative content of Si in the framework increased with time for the growth of the crystal grains. Up to 2.5 h, the relative content of Si in the framework achieved 80%. These give evidence that most Si atoms (80%) directly take part in the formation of the crystal nuclei as well as in the growth period of the crystal grains in the earlier stage (<2.5 h) of the crystallization in the forming of the Si(4Al) entities randomly. The slight increase of Si(4Al) and the appearance of the Si(3Al), Si(2Al), Si(1Al) and Si(0Al) after 2.5 h suggest that substitution of small amount of Si atoms for the phosphorus as well as for the phosphorus and aluminum pair takes place in the later stage of the crystallization to form small silica patches. But the increase of the relative content of Si in the earlier stage (<2.5 h) cannot rule out the common role of the substitution mechanism of P atoms. Therefore, we investigated the relative proportion of Si/Al/P

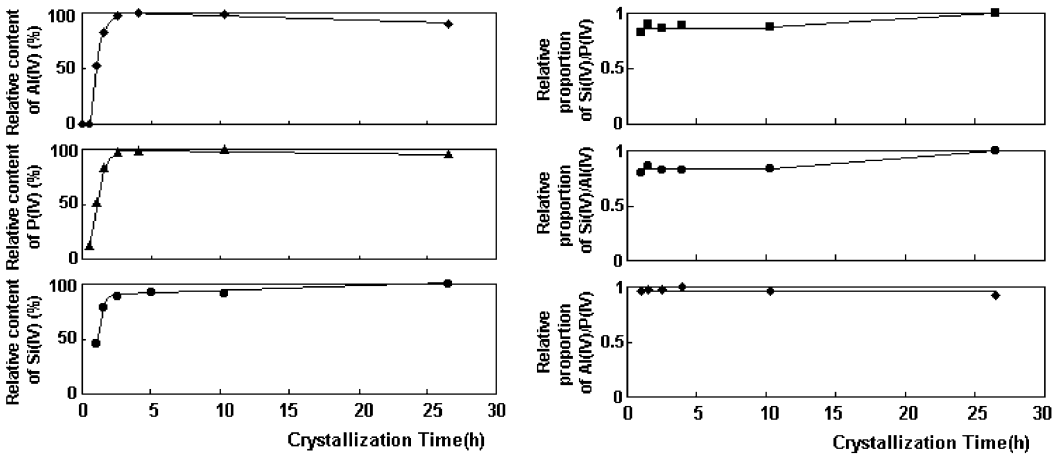

Fig. 11. Changes of the Al(IV), P(IV) and Si(IV) relative content (a) and relative proportion (b) of the as-synthesized samples with crystallization time.

incorporated into the framework of SAPO-34 (Fig. 11b). It showed clearly that the relative proportion of Al/P is basically balanced in the whole crystallization, and the same is true for Si/P and Si/Al in the early crystallization stage (>2.5 h). It reveals that Si, P and Al incorporate into the framework of SAPO-34 in a certain proportion and an equal rate in 2.5 h, which gives evidence that the major part of Si atoms (80%) incorporate into the framework by direct participation of the crystallization other than by the substitution for P in the earlier stage (<2.5 h). Whereas small amount of Si atoms (20%) incorporate by substitution mechanism in the later stage (>2.5 h). A model of the crystallization process of SAPO-34 is shown in Fig. 12.

3.6. Effect of Si incorporation on the acidity of the Brønsted acid sites

Fig. 13 showed the various possible Si environments in the SAPO-34 framework [17]. From our study of the Si incorporation mechanism, 80% Si atoms incorporate into the SAPO-34 framework as Si(4Al) entities (i.e. Fig. 13a) by the direct participation mechanism in the earlier stage (<2.5 h). It is easy to infer that these Si(4Al) entities should be isolated and well distributed in the framework, and these isolated Brønsted acid sites should be the main source of the acidity of SAPO-34. In the later stage (>2.5 h), small amount of Si atoms (20%) incorporate into the framework by the substitution mechanism, which cause the concentration of Si atoms as nonisolated Si(4Al) entities (i.e. Fig. 13b and c) and Si islands containing Si(nAl) ($n = 0$–3) structures (i.e. Fig. 13d–f). The number and the size of the Si-rich entities increase gradually with the crystallization time. The formation of these Si-rich entities promotes the acidity of SAPO-34, and that the acidity of the acid

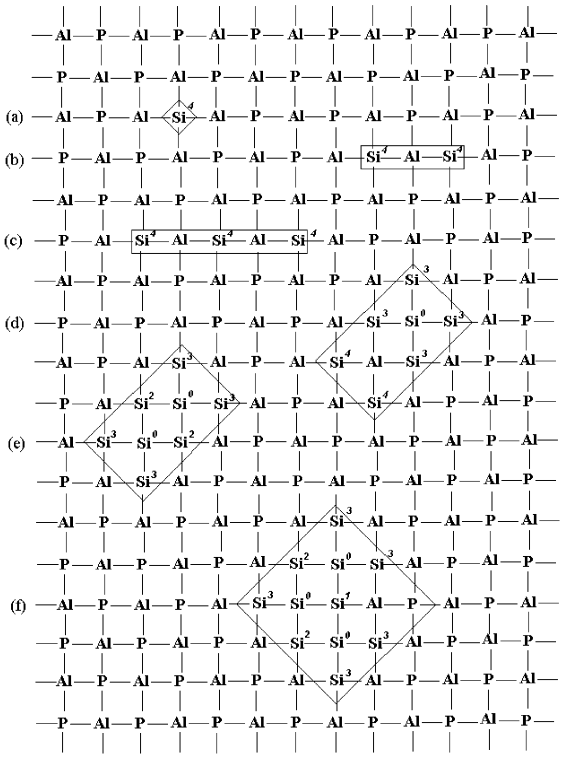

Fig. 13. Various possible Si environments in the SAPO-34 framework (4) Si(4Al) (3) Si(3Al) (2) Si(2Al) (1) Si(1Al) (0) Si(0Al).

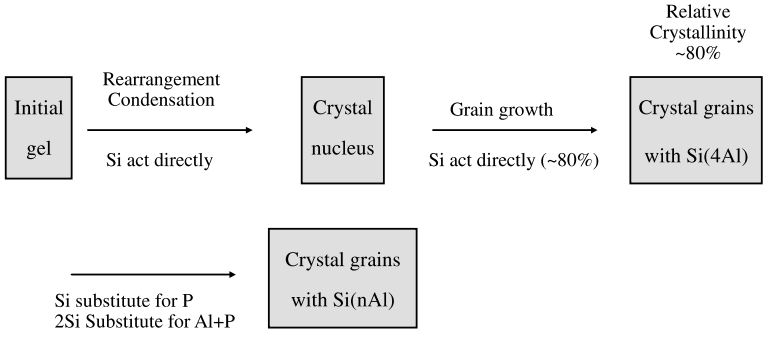

Fig. 12. A model of the SAPO-34 crystallization process.

centers at the edges of such islands will increase with island size [16]. The increase in acidity is primarily the result of the uneven distribution of the negative charges, which brings about by the substitution of Si for P and/or for Al and P. It should be noted that the changes on the structure of SAPO-34 in the crystallization process will directly lead to the change of acidity, and will certainly result in the differences in catalytic properties. These suggest the relations among acidity, structure and crystallization process, also the possibility to improve the acidity and catalytic properties, by choosing a optimum crystallization time, thus controlling the number and distribution of Si in the framework of SAPO-34.

4. Conclusions

In the previous work, we studied the whole crystallization of the small-pore molecular sieve SAPO-34 was monitored by various physicochemical techniques. Our results show that the whole crystallization process of SAPO-34 contained two stages, the earlier stage (<2.5 h) and the later stage (>2.5 h). In the first 2.5 h (the earlier stage), high up to ~80% of relative crystallinity could be achieved indicating a fast crystallization feature of the synthesis. It is revealed that the crystal nuclei of SAPO-34 result from the structure rearrangement of the initial gel and the condensation of the hydroxyls. The template and the ageing period are crucial for the later crystallization of SAPO-34. Preliminary structure units similar to the framework of SAPO-34 have already formed before the crystallization began (0 h and low temperature). Evidence shows that the formation of the SAPO-34 may be a type of gel conversion mechanism, the solution support and the appropriate solution circumstance are two important parameters of the crystallization of SAPO-34. The investigations of NMR have confirmed that the major part of the silicones (80%) incorporate into the SAPO-34 framework by direct participation of the crystallization other than by the substitution for P in the earlier stage (<2.5 h), form isolated and well-distributed Si(4Al) entities. While small amount of Si atoms (20%) incorporate into the framework forming small Si-rich entities by the substitution of the phosphorus as well as the phosphorus and aluminum pair in the later stage (>2.5 h). The close relations among acidity, structure and crystallization process are established, which provide the possibility to improve the acidity and catalytic properties by choosing a optimum crystallization time, thus controlling the number and distribution of Si in the framework of SAPO-34.

Acknowledgements

The authors are grateful to assistance of Wengui GUO in the IR, to Xingyun Huang in the XRD, to Meifang Jin in the SEM and to Jing Liu in the XRF measurements. Furthermore, they are indebted to Prof. Dongbai Liang and Dr. Yue Qi for valuable comments on the manuscript.

References

[1] B.M. Lok, C.A. Messina, P.R. Lyle, et al., US. 4, 440, 871, 1984.
[2] M.J.V. Niekerk, J.C.Q. Fletcher, C.T.O. Connar, Appl. Catal. A: Gener. 138 (1996) 135.
[3] A. Grønvold, K. Moljord, T. Dypvic, et al., Stud. Surf. Sci. Catal. 81 (1996) 399.
[4] J. Liang, H.Y. Li, S.Q. Zhao, W.G. Guo, et al., Appl. Catal. 64 (1990) 31–40.
[5] Y. Xu, C.P. Grey, J.M. Thomas, A.K. Cheetham, Catal. Lett. 4 (1990) 251.
[6] T. Inui, Stud. Surf. Sci. Catal. 105 (1997) 1441.
[7] T. Inui, Stud. Surf. Sci. Catal. 67 (1991) 233.
[8] S. Nawaz, S. Kolboe, S. Kvisle, et al., Stud. Surf. Sci. Catal. 61 (1991) 421.
[9] G. Cai, Z. Liu, R. Shi, et al., Appl. Catal. A: Gener. 125 (1996) 29–38.
[10] J. Chen, P.A. Wright, S. Natarajan, et al., Stud. Surf. Sci. Catal. 94 (1994) 1731.
[11] A.J. Marchi, G.F. Froment, Appl. Catal. 71 (1991) 139.
[12] K-H. Schnabel, R. Fricke, I. Girnus, et al., J. Chem. Soc. Faraday Trans. 87 (21) (1991) 3569.
[13] R.B. Borader, A. Clearfield, J. Mol. Catal. 88 (1994) 249–265.
[14] A.M. Parakash, S. Unnikrishnan, J. Chem. Soc. Faraday Trans. 90 (15) (1994) 2291.
[15] S. Ashtekar, S.V.V. Chilukuri, D.K. Chakrabarty, J. Phys. Chem. 98 (1994) 4878.
[16] G. Sastre, D.W. Lewis, C. Richard, A. Catlow, J. Phys. Chem. B 101 (27) (1997) 5249.

[17] R. Vomscheid, M. Briend, M.J. Peltre, et al., J. Phys. Chem. 98 (1994) 9614.
[18] E. Dumitriu, A. Azzouz, V. Hulea, et al., Microporous. Mater. 10 (1–3) (1997) 1.
[19] Z. Liu, G. Cai, C. He, Faming Zhuanli Gongkai Shenqing Shuomingshu CN1, 088, 483, 1994.
[20] M.W. Anderson, B. Sulikowski, P.J. Barrie, et al., J. Phys. Chem. 94 (1990) 2730–2734.
[21] C.S. Blackwell, R.L. Patton, J. Phys. Chem. 88 (1984) 6135.
[22] C.S. Blackwell, R.L. Patton, J. Phys. Chem. 92 (1988) 3965.
[23] Bodo Zibrowius, Elke Loffler Michael Hunger, Zeolites 12 (2) (1992) 167.
[24] E.J.P. Feijen, J.A. Martens, P.A. Jacobs, Stud. Surf. Sci. Catal. 84 (1994) 3.